Simple procedure for including vibrational effects in the calculation of electron-molecule cross sections

Wayne K. Trail, Michael A. Morrison, William A. Isaacs, and Bidhan C. Saha
Department of Physics & Astronomy, University of Oklahoma, Norman, Oklahoma 73019
(Received 21 September 1989)

The widely used rigid-rotor approximation of low-energy electron-molecule scattering theory neglects completely the vibrational motion of the target. The errors this approximation introduces into calculated elastic and rotational-excitation cross sections are larger than other sources of imprecision in present state-of-the-art electron-molecule collision studies. We have applied an alternative to the rigid-rotor approximation: an extremely simple vibrational averaging of the interaction potential. This procedure reintroduces effects due to the zero-point vibrational motion without incurring in the solution of the Schrödinger equation computational demands beyond those of a rigid-rotor calculation. Tests on e-H_2 and e-N_2 scattering demonstrate the improved accuracy and computational efficiency that results from vibrational averaging.

I. INTRODUCTION

The many degrees of freedom of the target in an electron-molecule collision—electronic, nuclear rotation, and nuclear vibration—pose computational challenges that have provoked theorists to design a variety of approximations to simplify scattering calculations.[1–3] In studies of *vibrationally elastic* processes (i.e., elastic scattering and rotational excitation within a particular electronic and vibrational state), the most widely used of these simplifications models the target molecule by a "microscopic dumbbell with electrons." This is the rigid-rotor (RR) approximation.

Operationally, this approximation amounts to fixing the target's internuclear separation R at its equilibrium value R_e. In such calculations, therefore, the vibrational motion of the nuclei is completely ignored; this gambit greatly reduces the computational chore of solving the Schrödinger equation. Hence the RR approximation appears in a variety of formulations of electron-molecule collision theory; e.g., in the $\underline{R}$-matrix, laboratory-frame close-coupling, body-frame fixed-nuclei (BFFN), and others.[2–4] While obviously of little use if vibrational excitation is of interest, in studies of elastic scattering and rotational excitation the RR approximation has become a mainstay.[1,5]

The price one pays for these simplifications is loss of accuracy. In e-H_2 scattering, for example, the RR approximation introduces error as large as 15% in rotational-excitation cross sections at energies below about 10 eV.[6] In state-of-the-art calculations, which aim to treat very accurately both the interaction potential and the collision dynamics, so large an error in unacceptable. While in principle one could fully incorporate the vibrational dynamics—in, for example, rovibrational close-coupling[7] or body-frame vibrational close-coupling calculations[8,9]—in practice doing so requires so much CPU time that it precludes study of complex molecules, such as CO_2, CH_4, or benzene.

One computationally viable alternative to full inclusion of rovibrational dynamics is an adiabatic treatment of the nuclear motion. In, for example, the adiabatic-nuclear-vibration (ANV) theory,[9,10] one calculates vibrational-excitation cross sections from RR scattering matrices (obtained by solving BFFN equations) at a discrete mesh of values of R. This method therefore requires solving RR equations at several values of R. Still, this method is much faster than a converged close-coupling treatment and produces elastic and rotational-excitation cross sections of greater accuracy than their RR counterparts.[11]

In solving RR scattering equations via a partial-wave expansion (in a single-center formulation), one faces an additional technical problem.[5] In order to converge the calculated cross sections, one must couple an artificially large number of angular momentum eigenstates of the projectile (the partial waves).[12–14] These high-order partial waves are unphysical because what couples them to the low-order partial waves—which *do* contribute to the cross section—is a singularity in the electrostatic interaction potential located a distance $R/2$ from the origin of coordinates. This off-center singularity is, of course, purely an artifice of the RR approximation; no such singularities occur in nature, where molecules vibrate. For large, highly aspherical molecules such as CO_2, the mere calculation of large-order harmonics that do not contribute to the cross section poses numerical difficulties.[12] But even for less extreme systems, this situation poses a practical difficulty. Because the computer time needed to solve the RR coupled radial differential equations increases as the square of the number of channels (or worse, depending on the algorithm[13]), inclusion of a large number of partial waves dramatically increases the time required to attain a desired precision.

We here propose a very simple alternative to the RR approximation for calculation of *vibrationally elastic* cross sections. This "vibrational-averaging" (VIBAV) procedure takes account of vibrational effects (approximately) but does not require either the coupling of vibra-

tional target states (as in a coupled-states method) or the solution of scattering equations with an unphysical singularity. To illustrate the procedure, we have applied it to the e-H_2 and e-N_2 systems; the former highlights the improved accuracy of VIBAV cross sections and the latter the improved computational efficiency for larger molecules with several electrons. In Sec. II we describe this simple technique as an approximation to coupled-states theory. In Sec. III we summarize details of our calculations and in Sec. IV discuss the results. Unless otherwise stated, atomic units are used throughout and the notation is that of Ref. 1

II. THEORY

A. VIBAV procedure

Off-center singularities in the RR electron-molecule potential arise from Coulomb interactions between the projectile and the nuclei. The scattering equation for electronically elastic collisions (assuming excited electronic states are omitted[1]) is just the projection of the full Schrödinger equation onto the (Born-Oppenheimer) electronic wave function of the ground state of the target; for H_2 this $X\,^1\Sigma_g^+$ state corresponds to a closed shell with configuration $1\sigma_g^2$. This projection leaves only the spatial variables of the internuclear axis $\mathbf{R}$ and the projectile $\mathbf{r}$. In the resulting "reduced" scattering equation, the two-particle bound-free Coulomb interactions are averaged over the ground state in the static potential term, which for e-H_2 is

$$V_{\rm st}(\mathbf{r},\mathbf{R})=\left\langle X\,^1\Sigma_g^+ \left| -\sum_{\mu=1}^{2}\frac{1}{|\mathbf{r}-\mathbf{R}_\mu|} + \sum_{i=1}^{2}\frac{1}{|\mathbf{r}-\mathbf{r}_i|}\right| X\,^1\Sigma_g^+\right\rangle . \quad (1a)$$

In practice, we calculate $V_{\rm st}(\mathbf{r},\mathbf{R})$ from the Hartree-Fock (HF) $1\sigma_g$ molecular orbital $\xi_{1\sigma_g}(\mathbf{r},R)$ as

$$V_{\rm st}(\mathbf{r},\mathbf{R})=-\sum_{\mu=1}^{2}\frac{1}{|\mathbf{r}-\mathbf{R}_\mu|} + \int \sum_{i=1}^{2}\frac{1}{|\mathbf{r}-\mathbf{r}_i|}|\xi_{1\sigma_g}(\mathbf{r}_i,R)|^2 d\mathbf{r}_i . \quad (1b)$$

In the matrix elements that appear in coupled-channel scattering equations [like Eqs. (3) below], there appear the Legendre projections of this potential. Using single-center coordinates with the origin at the center of mass of the molecule, we expand Eq. (1b) in Legendre polynomials as[15]

$$V_{\rm st}(\mathbf{r};\mathbf{R})=\sum_{\lambda}^{\lambda_{\max}} v_\lambda^{\rm st}(r;R)P_\lambda(\cos\theta) . \quad (2)$$

In practice one truncates this summation at a maximum order $\lambda_{\max}$ that is sufficient to converge the desired scattering quantities. The off-center singularity $\mathbf{r}=\mathbf{R}_\mu$ in the electron-nuclear term in Eqs. (1) manifests itself as a *cusp* at $r=R/2$ in each radial Legendre projection $v_\lambda^{\rm st}(r;R)$. Figures 1 and 2, for example, show the cusps in selected Legendre projections for e-H_2 and e-N_2.

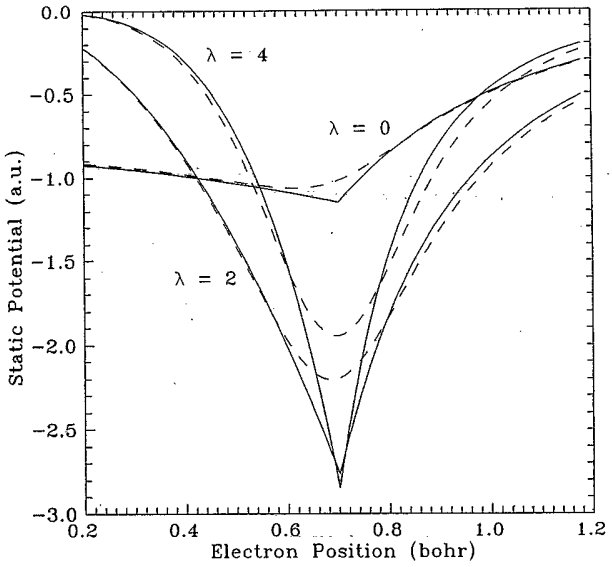

FIG. 1. Legendre projections $\lambda=0$, 2, and 4 of the static e-H_2 interaction potential [Eq. (2)]. The RR projections (solid curves) exhibit Coulomb cusps at $r=R/2$ that disappear when these projections are vibrationally averaged (dashed curves).

In RR matrix elements these cusps compound the convergence difficulties inherent in the nonspherical character of the interaction potential. For example, in a BFFN calculation[16] molecular vibrations are "frozen out" (via the RR approximation), while rotational effects are introduced asymptotically via the fixed-nuclear-orientation (FNO) approximation.[17] As its name implies, this approximation "freezes" the orientation of the internuclear

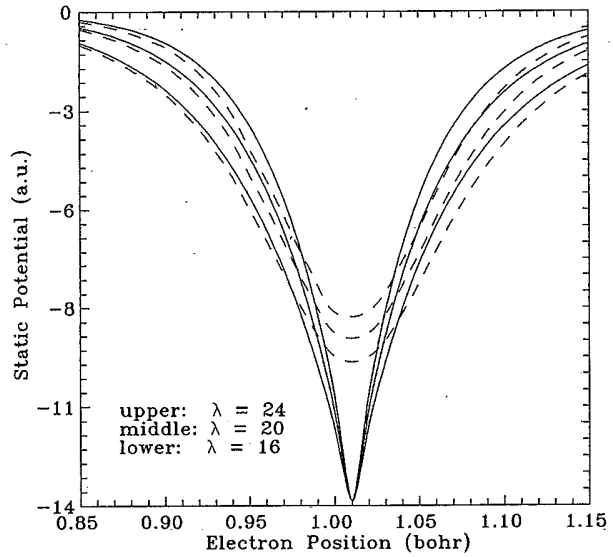

FIG. 2. Rigid-rotor (solid curve) and VIBAV (dashed curve) e-N_2 Legendre projections (with increasing magnitude) for $\lambda=16$, 20, and 24.

axis during the collision. The resulting Schrödinger equation is written in a body-fixed (BF) reference frame in which the z axis is coincident with the internuclear axis $\hat{\mathbf{R}}$. In this frame, the appropriate angular basis for reduction of the scattering equation to radial form is the set of spherical harmonics (i.e., partial waves) labeled by quantum numbers l and Λ, where l corresponds to the orbital angular momentum of the projectile and Λ to the projection of this observable along $\hat{\mathbf{z}}=\hat{\mathbf{R}}$. Projecting the scattering function onto this basis leads to the coupled equations[1,18]

$$\left[\frac{d^2}{dr^2}-\frac{l(l+1)}{r^2}+k_b^2\right]u^{\Lambda}_{l,l_0}(r;R) = 2\sum_{l'}[V^{\Lambda}_{l,l'}(r;R)+\hat{V}^{\Lambda}_{l,l'}(r;R)]u^{\Lambda}_{l',l_0}(r;R)\ . \quad (3)$$

In these equations R appears parametrically and so is offset by a semicolon. The matrix elements that couple partial waves come in two types: elements $V^{\Lambda}_{l,l'}(r)$ of local terms in the potential (e.g., static and local polarization terms) and elements $\hat{V}^{\Lambda}_{l,l'}(r)$ of nonlocal terms (e.g., exchange and nonlocal polarization-correlation terms). The caret on the second matrix element reminds us of its essentially nonlocal character [see Eq. (11) below].

Because cusps are present in the electron-nuclear part of each static matrix element, the solution of Eqs. (3) may require an enormous number of channels; e.g., in e-CO_2 scattering[12] one must couple as many as 32 channels, the actual number depending on the scattering energy and the electron-molecule symmetry (i.e., parity and value of Λ). Yet, in the BFFN T matrix $T^{\Lambda}_{ll_0}(R)$, one needs only elements corresponding to the lowest few partial waves to calculate accurate cross sections.

If one extends this RR treatment to include vibrational effects via the ANV approximation, the CPU time required by the cusps is aggravated by the need to solve RR scattering equations at several geometries. Doing so is necessary because the ANV transition amplitude for vibrational excitation is an integral (over R) of the BFFN T matrix with respect to initial-state and final-state vibrational wave functions: $\langle\phi_v|T^{\Lambda}_{ll_0}(R)|\phi_{v_0}\rangle$. For example, in a recent ANV study[9] of e-H_2 collisions we solved the RR equations for 11 values of R ranging from $0.7a_0$ to $2.6a_0$.

The offending cusps do not appear, however, in formulations that treat rigorously the dynamical effect of vibrations on the scattering function. For this reason it is useful to present the VIBAV procedure in the context of such a formulation. The best known of these is rovibrational laboratory-frame close-coupling (LFCC) theory.[7,19,20] But because we have implemented the VIBAV method in a body-fixed frame, we shall present it as an approximation to body-frame vibrational close-coupling (BFVCC) theory.[8,9]

The starting point for the BFVCC theory is an approximate treatment of rotations: working in the FNO approximation in the body frame, we neglect the rotational Hamiltonian in the Schrödinger equation and thus obtain the reduced Schrödinger equation

$$[T_e+\mathcal{H}_m^{(v)}+V_{\rm st}(\mathbf{r},R)+\hat{V}_{\rm ex}(\mathbf{r},R)-E]\times{}^{\rm FNO}\Psi^{\Lambda}_{E,v_0l_0}(\mathbf{r},R)=0\ , \quad (4)$$

where we label the reduced body-frame wave function ${}^{\rm FNO}\Psi^{\Lambda}_{E,v_0l_0}(\mathbf{r},R)$ by the total energy E and the vibrational and orbital angular momentum quantum numbers for the initial channel. Clearly, this formulation retains the dynamical effects of the vibrational Hamiltonian $\mathcal{H}_m^{(v)}$ on this function.

These effects appear as vibrational coupling when Eq. (4) is transformed via eigenfunction expansion into a set of coupled equations. The appropriate basis functions $\Phi^{\Lambda}_{vl}(\hat{\mathbf{r}},R)$ are products of eigenfunctions $\{\phi_v(R)\}$ of $\mathcal{H}_m^{(v)}$ and the aforementioned spherical harmonics $\{Y_l^{\Lambda}(\theta,\varphi)\}$, and the BFVCC expansion is

$${}^{\rm FNO}\Psi^{\Lambda}_{E,v_0l_0}(\mathbf{r},R)=\frac{1}{r}\sum_v\sum_l u^{\Lambda}_{vl,v_0l_0}(r)\Phi^{\Lambda}_{vl}(\hat{\mathbf{r}},R) \quad (5a)$$

$$=\frac{1}{rR}\sum_v\sum_l u^{\Lambda}_{vl,v_0l_0}(r)\phi_v(R)Y_l^{\Lambda}(\hat{\mathbf{r}})\ . \quad (5b)$$

When inserted into the FNO Schrödinger equation (4), this expansion leads to the BVFCC coupled integrodifferential equations

$$\left[\frac{d^2}{dr^2}-\frac{l(l+1)}{r^2}+k_v^2\right]u^{\Lambda}_{vl,v_0l_0}(r) = 2\sum_{v',l'}[V^{\Lambda}_{vl,v'l'}(r)+\hat{V}^{\Lambda}_{vl,v'l'}(r)]u^{\Lambda}_{v'l',v_0l_0}(r)\ . \quad (6)$$

Here the channel energy k_v^2 (in Rydbergs) corresponding to the radial function $u^{\Lambda}_{vl,v_0l_0}(r)$ is defined by energy conservation as the difference between E and the energy of the vth vibrational state,

$$\tfrac{1}{2}k_v^2=E-\epsilon_v\ . \quad (7)$$

The essential difference between the BFVCC equations (6) and the RR equations of BFFN theory (3) is the presence in the former of vibrational coupling. The integration over R implied by the static matrix element $V^{\Lambda}_{vl,v'l'}(r)$ in (6) "washes out" the offending cusps, and thus decreases the number of partial waves required for convergence.

In fact, *only* this integration—and not vibrational coupling *per se*—is required to eliminate the cusps. So if one is interested in vibrationally elastic scattering ($v=v_0$), one can simplify the BFVCC equations by truncating the *vibrational* expansion in (5) to a single term: the ground vibrational state. This reduces the coupled equations (6) to their *one-state* counterparts

$$\left[\frac{d^2}{dr^2}-\frac{l(l+1)}{r^2}+k_b^2\right]\bar{u}^{\Lambda}_{l,l_0}(r) = 2\sum_{l'}[\bar{V}^{\Lambda}_{l,l'}(r)+\bar{\hat{V}}^{\Lambda}_{l,l'}(r)]\bar{u}^{\Lambda}_{l',l_0}(r) \quad (8)$$

(Ref. 21). The overbar on the local and nonlocal matrix elements in (8) denotes that these are *vibrationally averaged* quantities. For example, the vibrationally averaged

static matrix element is

$$\bar{V}^{\Lambda}_{l,l'}(r)=\langle l\Lambda|\langle\phi_0|V_{\rm st}(\mathbf{r},R)|\phi_0\rangle|l'\Lambda\rangle \ . \tag{9}$$

By implementing the Legendre expansion (2), we can reduce the implied vibrational integral in (9) to a sum of simple averages over the probability density of the ground vibrational state; viz.,

$$\langle\phi_0|V_{\rm st}(\mathbf{r},R)|\phi_0\rangle = \sum_{\lambda}\left[\int_0^{\infty} v^{\rm st}_{\lambda}(r;R)|\phi_0(R)|^2R^2dR\right]P_{\lambda}(\cos\theta) \ . \tag{10}$$

One can easily evaluate these integrals by simple quadratures over a small mesh of values of R (see Sec. III).

The effect of vibrational averaging on the static Legendre projections is illustrated for e-H_2 and e-N_2 in Figs. 1 and 2. Figure 1 shows that in e-H_2, vibrational averaging acts on low-order static projections [i.e., small values of λ in Eq. (2)] mainly to eliminate the electron-nuclear cusps. But averaging also weakens slightly the minimum and widens slightly the "well" in each term; these alterations, however slight, do significantly improve the accuracy of rotational-excitation VIBAV cross sections over their RR counterparts (see Sec. IV).

Most electron-molecule systems are much more aspherical than e-H_2, so one must include Legendre projections of higher order in the expansion of the static potential. As illustrated in Fig. 2, these projections for e-N_2 (in the RR approximation) narrow with increasing λ and contain a cusp (of equal magnitude) at $r=R/2$. Vibrational averaging eliminates these cusps *and* significantly weakens each minimum—differences that are responsible for the increased computational efficiency of a VIBAV over a RR calculation for a system such as e-N_2 (see Sec. IV).

Operationally, the essential point for implementation of this procedure is that Eqs. (8) of the VIBAV method are *mathematically* identical to Eqs. (3) of BFFN theory. Hence one can use *without alteration* existing computer programs that solve the BFFN equations[22,23] by simply replacing RR Legendre projections in the BFFN matrix elements by the corresponding VIBAV projections (10).

One can, of course, implement vibrational averaging in other formulations of electron-molecule collision theory. For example, in the rotational LFCC method, one merely replaces $v^{\rm st}_{\lambda}(r;R_e)$ in the coupling matrix elements[24] $V^{J}_{jl,j'l'}$ by their vibrational averages.

However it is formulated, the VIBAV method remains a one-state approximation and thus neglects coupling to (open and closed) excited vibrational states [$v'>0$ in the sum in Eqs. (6)]; the extent to which this approximation affects vibrationally elastic cross sections depends on the system and scattering energy being studied. But in any case VIBAV cross sections will be at least as accurate as RR results, which ignore vibrational effects altogether.

B. Further simplifications: The nonlocal potential

The potential in the VIBAV equations (8) includes contributions from static, exchange, and polarization-correlation interactions. Since the singularity in the Coulomb potential appears only in the (electron-nuclear) static term, one can simplify further the VIBAV scattering calculations (while incurring very little loss of accuracy) by averaging *only* that term. For example, it is particularly useful to approximate nonlocal operators in the potential by their equilibrium values.

For many systems, exchange or correlation effects can be accurately represented by local model potentials,[25,26] but if such models are inapplicable or inappropriate, then the nonlocality of these effects markedly complicates the solution of scattering equations. For example, the exchange operator in the BFVCC coupled equations for e-H_2 scattering [Eqs. (6)] acts on one component of the radial function as

$$\hat{V}_{\rm ex}(\mathbf{r},R)u^{\Lambda}_{v'l',v_0l_0}(r)=\int_0^{\infty}K^{\Lambda}_{vl,v'l'}(r,r')\times u^{\Lambda}_{v'l',v_0l_0}(r')dr' \ , \tag{11}$$

where the BFVCC exchange kernel is

$$K^{\Lambda}_{vl,v'l'}(r,r')=rr'\int\Phi^{\Lambda}_{vl}(\hat{\mathbf{r}},R)^*\left[\xi_{1\sigma_g}(\mathbf{r},R)\frac{1}{|\mathbf{r}-\mathbf{r}'|}\xi_{1\sigma_g}(\mathbf{r}',R)\right]\Phi^{\Lambda}_{v'l'}(\hat{\mathbf{r}}',R)d\hat{\mathbf{r}}\,d\hat{\mathbf{r}}'dR \ . \tag{12}$$

Although exchange significantly influences low-energy electron-molecule cross sections,[27] the exchange operator varies weakly with R over the region of the ground-state vibrational probability density $|\phi_0(R)|^2$. So approximating the matrix elements $\bar{V}^{\Lambda}_{l,l'}(r)$ in Eqs. (8) by their equilibrium values $\hat{V}^{\Lambda}_{l,l'}(r;R_e)$ should be an excellent approximation. Similarly one can approximate the polarization interaction—another bound-free electron-electron effect—by its equilibrium value, as illustrated by the e-N_2 calculations reported in Sec. IV B.

III. DESCRIPTION OF THE CALCULATIONS

A. H_2 and N_2 interaction potentials

We calculate the static, exchange, and polarization components of the interaction potentials for both systems from near-Hartree-Fock electronic ground-state wave functions on a grid of internuclear separations R determined by the probability density of the ground vibrational state. As Fig. 3 shows, this range is more compact for N_2 than for H_2.

To obtain these electronic functions, we solve the electronic Schrödinger equation of the molecule variationally[28] using symmetry-adapted bases of contracted nucleus-centered Gaussian-type orbitals. These bases include compact polarization functions that allow for bond formation[29] in the neutral molecule; when used to determine the polarization potential described below, each basis is augmented by additional diffuse functions to allow for distortion of the neutral by the scattering electron. The R variation of the electronic wave functions is carried entirely by the linear variational parameters.

For e-H_2 we use a (5*s*2*p*/3*s*2*p*) basis for the neutral and

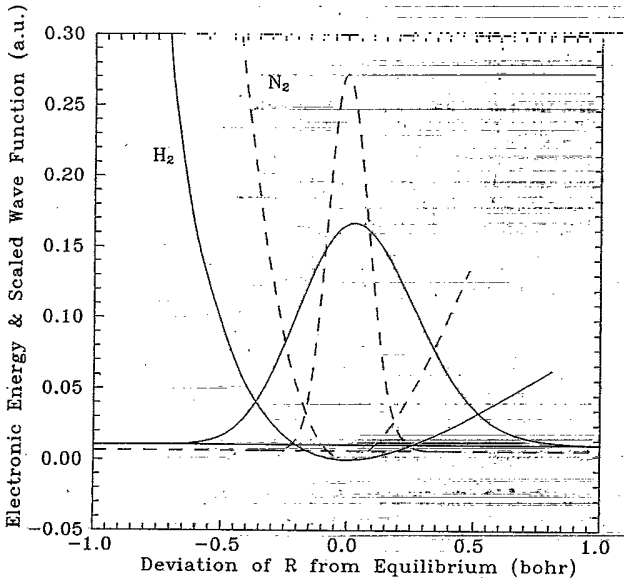

FIG. 3. Ground-state $X\,^1\Sigma_g^+$ near-HF potential energy curves and associated ground-state vibrational wave functions for H_2 (solid curves) and N_2 (dashed curves). To facilitate comparisons (see Sec. III) all curves are plotted as a function of $R-R_e$ and the electronic energies (plus the internuclear repulsion potential) are plotted as $\mathcal{E}^{(e)}(R)-\mathcal{E}^{(e)}(R_e)$. The vibrational wave functions were calculated by solving the nuclear Schrödinger equation (13) as described in Sec. III C and are here scaled by $\frac{1}{10}$ and plotted on a horizontal axis chosen to indicate the corresponding vibrational energy: $\varepsilon_0=0.0104E_h$ for H_2 and $\varepsilon_0=0.0062E_h$ for N_2.

a $(6s3p/4s3p)$ basis for the polarized molecule. The exponents and contraction coefficients for these bases appear in Table I of Ref. 30. For e-N_2, we use the $(9s5p1d/5s3p1d)$ neutral basis of Ref. 31 and augment this basis to allow for polarization as described in Sec. III A of Refs. 32 and 33.

Figure 3 shows the electronic energy curves for the ground states of N_2 and H_2. At equilibrium, our electronic energies are $-1.132\,895E_h$ for H_2 and $-108.974\,556E_h$ for N_2; the corresponding Hartree-Fock (HF) limits are[34] $-1.133\,63E_h$ and[35] $-108.9928E_h$, respectively.[36]

Important properties of these electronic wave functions are their permanent and induced moments. In particular, accurate calculation of low-energy cross sections requires wave functions that yield accurate values for at least the permanent quadrupole moment (q), spherical polarizability (α_0), and nonspherical polarizability (α_2). In Table I we compare our near-HF values for these moments, averaged over the ground vibrational state of the target, with corresponding experimental values.[37–41] As discussed in Sec. III C, we calculate these averaged moments from the vibrational wave functions that solve the appropriate nuclear Schrödinger equation with the potential energy curves of Fig. 3.

We calculate the static potential (1b) and the exchange kernel (12) from the bound $1\sigma_g$ orbital of the neutral. In solving the BFFN scattering equations (3), either for RR or VIBAV studies, we can treat this kernel directly.[42] In

TABLE I. Properties of the ground $X\,^1\Sigma_g^+$ states of H_2 and N_2 as determined from wave functions used in the present scattering calculations.

Property	Near HF	Expt.
	e-H_2	
$\langle\phi_0\|q(R)\|\phi_0\rangle$	−0.4704	−0.474±0.034[a]
$\langle\phi_0\|\alpha_0(R)\|\phi_0\rangle$	5.376	5.4265[b,c]
$\langle\phi_0\|\alpha_2(R)\|\phi_0\rangle$	1.410	1.3567[b,a]
	e-N_2	
$\langle\phi_0\|q(R)\|\phi_0\rangle$	−0.962	−1.04±0.07[d]
$\langle\phi_0\|\alpha_0(R)\|\phi_0\rangle$	11.493	11.744±0.004[c,e]
$\langle\phi_0\|\alpha_2(R)\|\phi_0\rangle$	3.30	3.08±0.002[d,e]

[a]Reference 37.
[b]Reference 38.
[c]Reference 39.
[d]Reference 40.
[e]Reference 41.

solving the BFVCC equations (6), however, we represent the kernel via a separable expansion[43] using an exchange basis consisting of bound and virtual molecular orbitals from the aforementioned structure calculations. Details of our use of a separable representation of the exchange kernel in BFVCC calculations will appear elsewhere.[44]

The final component of our interaction potential accounts for (long-range) polarization and (short-range) correlation effects with a local, energy-independent potential. This function includes all *adiabatic* polarization effects exactly via linear variational calculations on the polarized and unpolarized target. (Refs. 30 and 31 detail the calculation of these potentials for e-H_2 and e-N_2, respectively). This potential allows for nonadiabatic (correlation) effects via a nonpenetrating approximation[45] according to which the two-electron bound-free electrostatic interactions are set to zero whenever the radial coordinate of the projectile is less than that of the one-particle density function of the target.

For both systems considered here, this potential can be very accurately represented by the *dipole* term in the moment expansion of this potential;[46] hence we have adopted the forms christened by Gibson and Morrison[30,46] the "better than adiabatic dipole" (BTAD) potential. Unlike the widely used semiempirical heuristic polarization potentials,[5] which account for short-range effects via a cutoff function that includes an adjustable parameter, the BTAD potential is parameter-free. Analytic forms for the equilibrium BTAD potentials for e-H_2 and e-N_2 are given in Eqs. (6) and (7) of Ref. 47 and Eqs. (21) of Ref. 32, respectively. From the asymptotic form of this potential at each R we extract the polarizabilities $\alpha_0(R)$ and $\alpha_2(R)$ in Table I.

B. Solution of the scattering equations

To obtain benchmark cross sections we solve the coupled integrodifferential BFVCC scattering equations (6), including exchange via the separable representation described above. To do so we apply an integral equations algorithm in which standard Green's functions are used to convert Eqs. (8) to a set of integral equations. These

equations are then solved via numerical quadrature; details of our implementation of this algorithm and an extensive set of references appear in Refs. 12 and 13.

To obtain RR and VIBAV results, we solve the BFFN equations (3). In solving these equations, since R is fixed at R_e, it is feasible to treat exchange directly, and we do so in several of the calculations reported in Sec. IV. We use the linear algebraic method of Schneider and Collins[48] according to which Eqs. (3) are first transformed into integral equations that incorporate scattering boundary conditions via a Green's function. Subsequent imposition of simple quadratures on all integrals further transforms these equations to a set of simultaneous linear algebraic equations that are ideal for vectorization and efficient solution on a supercomputer.

In both sets of calculations we converged all integrated cross sections and eigenphase sums to better than 1%. To do so for e-H_2 we included (in both BFVCC and BFFN calculations) six partial waves in the Σ_g, Σ_u, and Π_u symmetries and five partial waves in the Π_g and Δ_g symmetries. We integrated all coupled e-H_2 equations to $170a_0$. In the vibrationally coupled BFVCC e-H_2 calculations we included four vibrational states.

To converge our Σ_g e-N_2 calculations we included 32 partial waves and integrated the coupled equations to $85a_0$. (For more details on the RR and VIBAV e-N_2 calculations see Sec. IV B.)

Finally, in the expansions (2) of the static potential for both systems we include terms up to $\lambda_{\max}$ equal to twice the maximum order partial wave required for convergence. Note that for e-N_2, the electron-nuclear terms dominate the high-order static Legendre projections (see Fig. 2).

C. Evaluation of vibrational wave functions

For both BFVCC and VIBAV calculations we require vibrational wave functions of the target. Since the ground-state potential of N_2 (Fig. 3) is deep, narrow, and nearly symmetric, one could approximate these functions by eigenfunctions of the simple harmonic oscillator (SHO) Hamiltonian using the natural frequencies in tables such as those in Ref. 49. But in H_2 these conditions are not met (see Fig. 3) and one must solve the nuclear Schrödinger equation numerically using as a potential the HF $X\,^1\Sigma_g^+$ electronic energy. In the event, we solved this equation for both systems.

To simplify the solution of the nuclear Schrödinger equation we neglect vibrational-rotational coupling, i.e., we replace the centrifugal potential by its equilibrium value. Thus the equation for vibrational eigenfunctions $\phi_v(R)$ with energies ε_v is

$$\left[\frac{d^2}{dR^2}+V_{nn}(R)+\mathcal{E}_0^{(e)}(R)-\varepsilon_v\right]\phi_v(R)=0\ , \tag{13}$$

where V_{nn} is the potential of internuclear repulsion. Operationally, we begin by fitting the potential energy in this equation to a Simons-Parr-Finlan-Dunham form[50]

$$\mathcal{E}_0^{(e)}(R)+V_{nn}=b_0r^2\left[1+\sum_{i=1}^{n}b_ir^i\right]-\epsilon\ , \tag{14}$$

where ϵ is the depth of the potential well and $r\equiv(R-R_e)/R$. We then solve (13) via the linear variational method, expanding the vibrational wave function $\phi_v(R)$ in a basis of SHO eigenfunctions and diagonalizing the resulting matrix of the vibrational Hamiltonian. In practice, we can save considerable CPU time by evaluating the desired wave functions at the points of a Gauss-Hermite quadrature[51] whose points are the values of R we will subsequently need to evaluate vibrational matrix elements and averages in scattering equations.

IV. RESULTS

A. e-H_2 collisions

Compared to other molecules, hydrogen is nearly spherical. So converging e-H_2 coupled-channel calculations requires only a few partial waves whether or not one implements the RR approximation (see Sec. III). Under these special circumstances, elimination of the Coulomb cusps saves little CPU time. But vibrational effects significantly influence e-H_2 cross sections, particularly those for rotational excitation.

The VIBAV transition matrix $\bar{T}^{\Lambda}_{l,l_0}$ approximates the $v_0=v=0$ block of the full BFVCC matrix T^{Λ}_{vl,v_0l_0}. Therefore VIBAV (and RR) cross sections approximate *vibrationally elastic* BFVCC cross sections, e.g., those determined in vibrationally converged calculations described in Sec. III. (Since the FNO approximation is implicit in the BFVCC formulation, these cross sections are equivalent to the sum of the elastic and all rotational excitation cross sections.[52])

Before examining the effect of various approximate treatments of the vibrational motion, we shall consider the exchange kernel. As noted in Sec. II B, in many of our calculations we expand this kernel in a separable representation. In Fig. 4(a) we compare vibrationally elastic cross sections based on such a representation with those from calculations in which exchange effects are treated exactly. We obtain the vibrationally averaged–static, exchange, and polarization (VIBAV-SEP) results in this figure by vibrationally averaging all three constituents of the interaction potential—static, exchange, and polarization—and expanding the kernel. The exact-exchange cross sections in this figure derive from *adiabatic nuclei* calculations, i.e., from vibrationally averaged $\underline{T}$ matrices obtained from solution of the BFFN equations (3) at 11 values of R (see Sec. II A).

Also noted in Sec. II B was the idea of simplifying VIBAV calculations by approximating the exchange kernel (12) by its equilibrium value. This simplification produces vibrationally averaged–static and polarization (VIBAV-SP) results, which can be seen in Fig. 4(a) to closely parallel those of the VIBAV-SEP and ANV calculations.

Figure 4(b) shows the effects of various treatments of vibrational motion on these e-H_2 elastic cross sections.

As benchmarks for these comparisons we use cross sections from BFVCC calculations that are fully converged in vibrational states (and partial waves). [In these as in all calculations in Fig. 4(b), we use the separable representation of the exchange kernel.] Except for a slight shift in the position of the enhancement at 3.0 eV, the VIBAV-SEP results agree well with these benchmarks. It is hardly surprising that the effects of the R variation of the exchange kernel are greatest near 3.0 eV: this sensitivity should be greatest near a shape resonance, where localization of the scattering function near the target enhances exchange effects. [See, in this regard, Fig. 6(a)]. The further approximation of treating exchange at equilibrium, which yields the VIBAV-SP numbers in this figure, induces only small additional changes in these cross sections.

One can simplify the VIBAV procedure even further by replacing the polarization potential by its equilibrium value, leaving only the static interaction to be vibrationally averaged. The resulting vibrationally averaged–static (VIBAV-S) cross sections in Fig. 4(b) show that the effect of doing so is negligible: these results differ from those obtained with full R variation of the polarization potential (the VIBAV-SP curve) by less than 1%.

Finally, we note that equilibrium approximations to

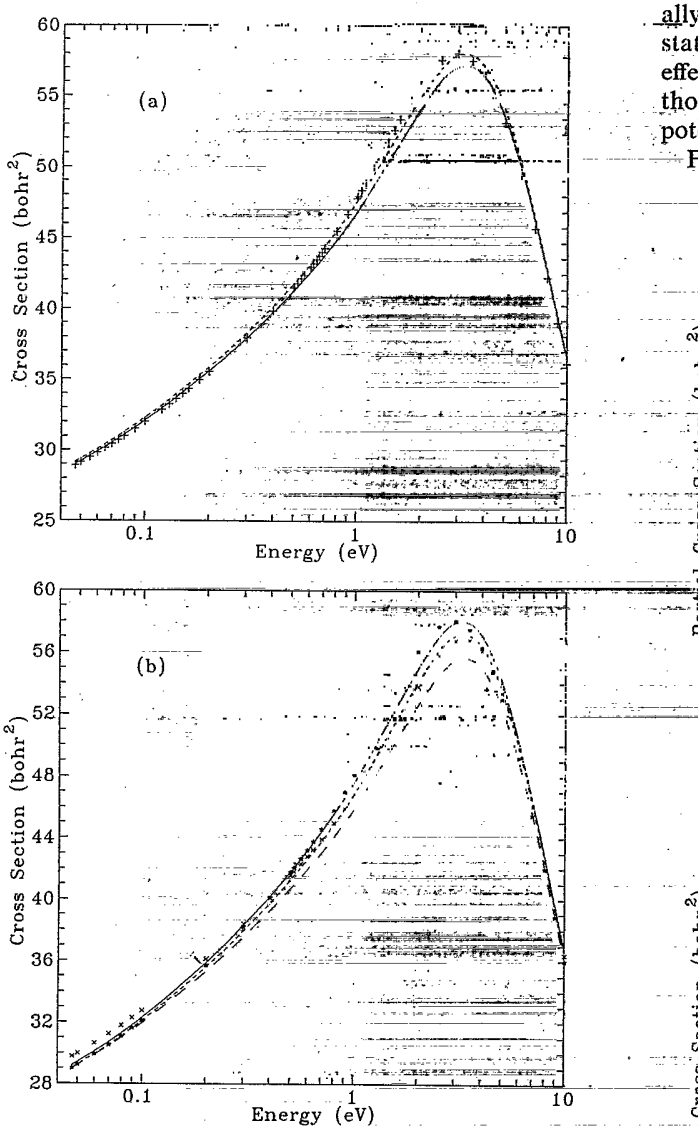

FIG. 4. Various treatments of (a) exchange and (b) the vibrational dynamics in the calculation of vibrationally elastic e-H_2 cross sections. In (a) results from VIBAV-SEP (solid curve) and VIBAV-SP (short-dashed curve) studies, in which the exchange kernel is expanded in a 132-function separable basis, are compared to (benchmark) ANV cross sections (pluses) from calculations in which exchange is treated exactly, as described in Sec. II. In (b) fully converged (benchmark) BFVCC cross sections (stars) are compared to VIBAV-SEP (solid curve), VIBAV-SP (short-dashed curve), VIBAV-S (crosses), and RR (long-dashed curve) results—all of which were calculated using the aforementioned separable expansion of the exchange kernel.

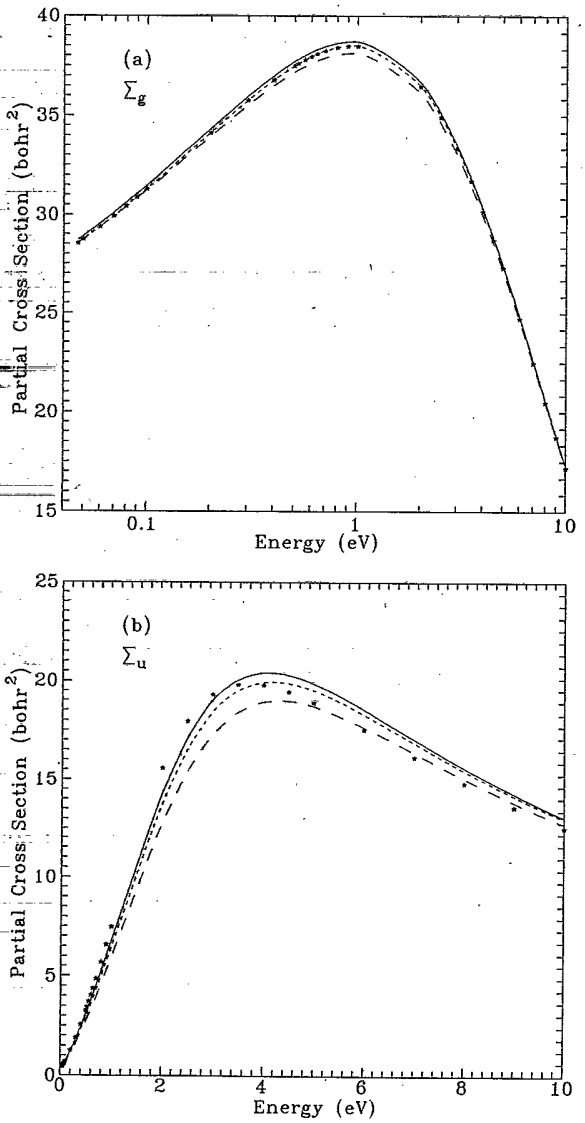

FIG. 5. Partial e-H_2 cross sections in the (a) Σ_g and (b) Σ_u symmetries from calculations using the VIBAV-SEP (solid curve), VIBAV-SP (short-dashed curve) and RR (long-dashed curve) approximations. Also shown are fully converged BFVCC results (stars).

electron-electron interactions such as exchange and polarization should be *more* accurate for most molecules than for H_2. For example, because of the comparative narrowness of the N_2 potential energy curve (Fig. 3), the excursions of the nitrogen nuclei from equilibrium (in, say, the ground vibrational state) are less than those of H_2, so equilibrium-exchange and -polarization approximations should be correspondingly more accurate for the larger system. (See Sec. IV B for illustrative VIBAV-S e-N_2 results.)

The agreement of VIBAV vibrationally elastic cross sections and converged BFVCC results shows that for this scattering process the coupling of the ground vibrational state to states with $v>0$ is comparatively unimportant; i.e., the one-state approximation is excellent. One might also conclude from this figure that the RR approximation is adequate for this system. But this conclusion is not correct for all scattering processes.

To see why, we turn to partial cross sections in various electron-molecule symmetries. In Figs. 5 we examine the dominant partial cross sections, those in the Σ_g and Σ_u symmetries. These cross sections and the corresponding eigenphase sums (given at selected energies in Table II) show that vibrational effects are far greater in the Σ_u symmetry than in the Σ_g symmetry. At low energies, elastic scattering is primarily Σ_g in character, so elastic cross sections show minimal vibrational effects (*vidé* Figs. 4). But rotational excitation is dominated by Σ_u, so the differences between RR and VIBAV cross sections should be more pronounced for this process.

Figures 6 show that this is indeed the case. Figure 6(a) displays the $j_0=0\rightarrow j=2$ e-H_2 cross section, $\sigma_{0\rightarrow 2}$, as determined from BFVCC, VIBAV-SEP, VIBAV-SP, and RR T matrices via the scaled adiabatic-nuclear-rotation approximation.[53] From threshold (44.1 meV) to about 2.0 eV, the error in $\sigma_{0\rightarrow 2}$ due to the RR approximation ranges from 8% to 15%; from 2.0 eV to 10 eV, this error is from 4% to 5%. The corresponding VIBAV cross sections at all energies are accurate to better than 5%; at energies above 1.0 eV they are accurate to better than 1% (see also Table III). One finds similar improvement in the $j_0=1\rightarrow j=3$ cross section.[54]

TABLE II. e-H_2 eigenphase sums at selected energy as calculated in the VIBAV-SP (upper values) and RR (lower values) approximation. In both sets of calculations, exchange was included exactly (at equilibrium) and polarization via the BTAD potential (see text). ($1.0[-2]=1.0\times10^{-2}$.)

E (eV)	Σ_g	Σ_u	Π_u	Π_g
0.047	3.056	1.164[−2]	1.788[−3]	1.541[−3]
	3.055	1.118[−2]	1.754[−3]	1.473[−3]
0.05	3.053	1.224[−2]	1.991[−3]	1.632[−3]
	3.052	1.175[−2]	1.952[−3]	1.561[−3]
0.07	3.034	1.608[−2]	3.379[−3]	2.209[−3]
	3.034	1.544[−2]	3.307[−3]	2.117[−3]
0.1	3.011	2.169[−2]	5.534[−3]	2.942[−3]
	3.010	2.083[−2]	5.412[−3]	2.821[−3]
0.5	2.820	1.003[−1]	3.874[−2]	1.165[−2]
	2.820	9.626[−2]	3.798[−2]	1.122[−2]
1.0	2.674	2.106[−1]	8.214[−2]	2.118[−2]
	2.675	2.019[−1]	8.074[−2]	2.042[−2]
2.0	2.477	4.426[−1]	1.653[−1]	3.929[−2]
	2.480	4.248[−1]	1.631[−1]	3.794[−2]
3.0	2.338	6.457[−1]	2.378[−1]	5.681[−2]
	2.341	6.220[−1]	2.351[−1]	5.492[−2]
4.0	2.230	7.994[−1]	2.980[−1]	7.383[−2]
	2.233	7.733[−1]	2.951[−1]	7.148[−2]
6.0	2.069	9.858[−1]	3.863[−1]	1.061[−1]
	2.072	9.603[−1]	3.832[−1]	1.030[−1]
8.0	1.951	1.081	4.438[−1]	1.356[−1]
	1.954	1.057	4.408[−1]	1.318[−1]
10.0	1.859	1.132	4.819[−1]	1.624[−1]
	1.863	1.111	4.790[−1]	1.581[−1]

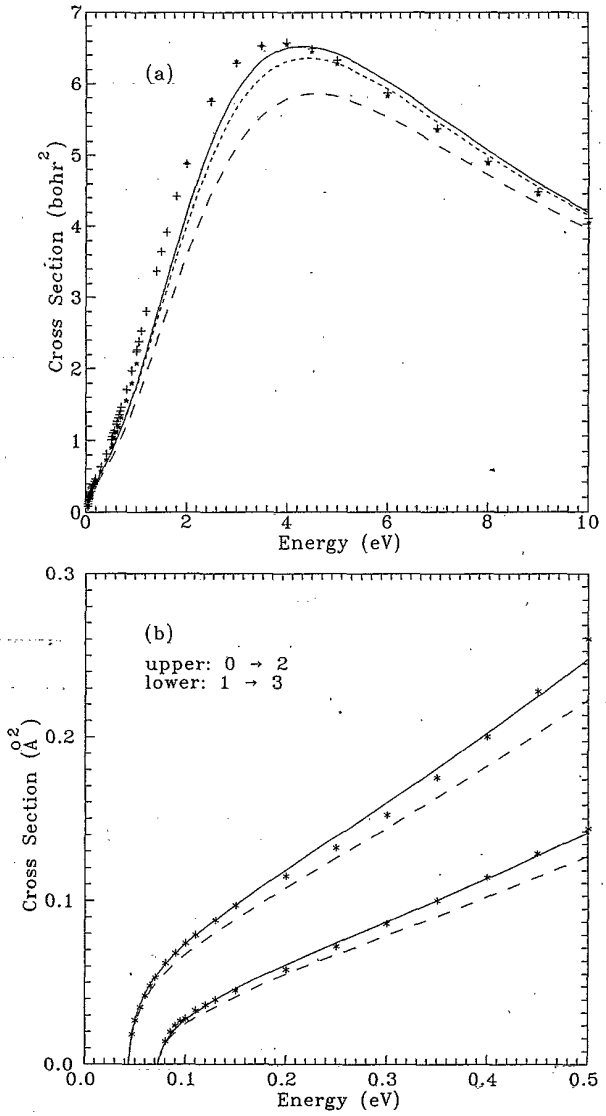

FIG. 6. (a) Approximations in the calculation of rotational excitation ($0\rightarrow2$) e-H_2 cross sections. Results from BFVCC (stars), VIBAV-SEP (solid curve), VIBAV-SP (short-dashed curve), and RR (long-dashed curve) calculations are based on a separable expansion of the exchange kernel. Also shown are ANV cross sections (pluses), for which exchange is treated exactly. In (b) VIBAV-SP (solid lines) and RR cross sections for the $0\rightarrow2$ and $1\rightarrow3$ excitations are compared to experimental (swarm-derived) data (stars) from Ref. 55.

TABLE III. e-H_2 cross sections (in square bohr) at selected energies (in eV) from benchmark converged BFVCC calculations (top line), VIBAV-SP calculations (second line), and RR calculations (third line). In all cases, exchange was included exactly at equilibrium.

E	$\sigma_{0\to0}$	$\sigma^M_{0\to0}$	$\sigma_{0\to2}$	$\sigma_{1\to3}$
0.05	29.201	32.115	0.103	
	28.647	31.543	0.098	
	28.677	31.477	0.090	
0.07	30.430	34.057	0.195	
	29.929	33.536	0.190	
	29.914	33.395	0.174	
0.10	31.861	36.372	0.265	0.099
	31.441	35.930	0.263	0.097
	31.368	35.698	0.240	0.089
0.50	40.178	51.674	0.874	0.498
	40.146	51.683	0.886	0.505
	39.682	50.793	0.795	0.453
1.00	44.834	60.484	1.920	1.152
	45.001	60.745	1.886	1.106
	44.251	59.436	1.681	0.986
2.00	50.120	65.743	4.294	2.576
	50.475	66.303	4.325	2.595
	49.402	64.833	3.865	2.319
3.00	51.609	61.654	5.987	3.592
	52.005	62.227	6.026	3.616
	50.947	61.146	6.450	3.270
4.00	50.251	53.979	6.576	3.946
	50.607	54.482	6.629	3.977
	49.738	53.844	6.075	3.645
6.00	44.158	39.208	6.050	3.631
	44.435	39.584	6.103	3.662
	43.929	39.430	5.703	3.422
8.00	37.737	28.841	5.084	3.052
	38.010	29.127	5.105	3.063
	37.709	29.129	4.824	2.895
10.00	32.303	21.930	4.255	2.554
	32.582	22.129	4.257	2.555
	32.394	22.179	4.052	2.432

In Fig. 6(b) we compare RR and VIBAV-SP cross sections for both excitations to experimental values derived from transport coefficients measured in swarm experiments.[55] And, for completeness, we show in Fig. 7 how RR, VIBAV and BFVCC total cross sections compare to recent experimental data.[56–58]

B. e-N_2 collisions

The greater asphericity of the nitrogen molecule makes converging e-N_2 scattering calculations considerably more difficult than doing so for e-H_2. Far more coupled partial waves are required,[13] so the effect of the off-center Coulomb singularity is correspondingly greater. Hence *removal* of these cusps results in a greater saving in CPU time.

Partial wave coupling is greatest in the Σ_g partial cross section[32] (because the Σ_g T matrix admits even-parity angular momentum scattering states beginning with the fully penetrating $l=0$ wave). To study the effects of vibrational averaging on partial-wave coupling in the e-N_2 system we have therefore focused on this symmetry, calculating Σ_g RR, VIBAV-S, and (converged) BFVCC cross sections. In these calculations, exchange effects were represented via the tuned free-electron-gas potential[25] at equilibrium. Figure 8 shows that in this symmetry the RR approximation introduces errors as large as 16% at 0.01 eV; by contrast, the VIBAV cross section at this energy is accurate to 4%.

The CPU time required to converge these cross sec-

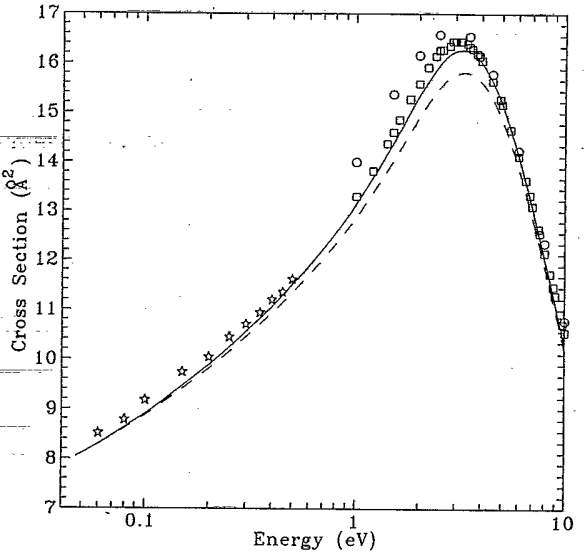

FIG. 7. Total e-H_2 cross sections in the VIBAV-SP (solid curve) and RR (dashed curve) theories compared to experimental results of Ferch (Ref. 56) (stars), Dalba *et al.* (Ref. 57) (open circles), and Jones (Ref. 58) (open squares). (Exchange was treated exactly in all calculations.)

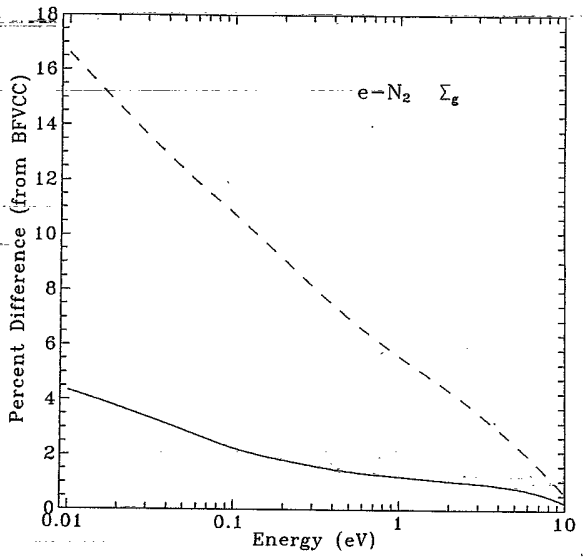

FIG. 8. Analysis of the accuracy of partial e-N_2 cross sections in the Σ_g symmetry: percent difference of VIBAV-S (solid curve) and RR (dashed curve) cross sections from converged BFVCC results.

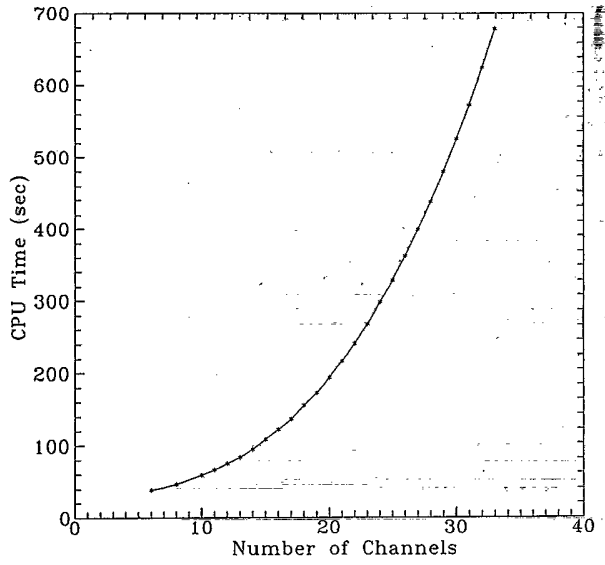

FIG. 9. Dependence of CPU time (on a MicroVax II computer) on number of channels (partial waves) for solution of the BFFN scattering equations (3) using the integral equations method (Ref. 13). For this illustrative case, the e-N_2 Σ_g equations were solved using a local exchange potential (Ref. 25).

tions increases dramatically with the number of coupled partial waves. Figure 9 illustrates this effect for the BFFN radial scattering equations (3). But because the VIBAV procedure eliminates the e-N_2 Coulomb cusps (Fig. 2), it decreases the number of partial waves required to attain a specified degree of convergence. For example, to calculate RR Σ_g cross sections at 0.01 eV accurate to 1% requires 32 channels; to calculate the corresponding VIBAV cross sections requires only 28 channels. This reduction translates into a saving in computer time of approximately 40%. In particular, Table IV shows the CPU time needed to calculate RR and VIBAV cross sections to various degrees of convergence. Note that because of the strong dependence of CPU time on number of channels (Fig. 9), the savings introduced by the VIBAV method *increases* with the desired precision.

V. CONCLUSION

The computational difficulty of fully converging a vibrational close-coupling calculation has often led to the omission of the nuclear Hamiltonian from the Schrödinger equation, i.e., the RR approximation. Averaging the interaction potential over the ground vibrational state restores the zero-point nuclear motion and thereby approximates effects that are completely ignored otherwise. Implementing the VIBAV procedure requires only writing a program for simple radial quadratures over R [Eq. (10)]; one need not modify the far more complicated programs that solve RR scattering equations. In fact, for most electron-molecule systems, solution of the VIBAV equations actually requires *less* CPU time than solving the corresponding RR equations.

TABLE IV. CPU times in seconds (on a MicroVax II computer) for calculation of e-N_2 cross sections in the Σ_g symmetry to the indicated degree of convergence.

Convergence (%)	RR	VIBAV
1	297	208
5	108	85
10	75	66

These improvements result from elimination of cusps in the electron-nuclear Coulomb interaction. Other terms in the potential reflect electron-electron interactions, and one can further simplify the VIBAV procedure by approximating these terms by their equilibrium values. Such simplifications are particularly desirable if the interaction is nonlocal, e.g., exchange.

In e-H_2, vibrational averaging changes both elastic and rotational-excitation cross sections. But because vibrational effects for this system are most pronounced in the Σ_u symmetry, the improvements of VIBAV over RR values are greatest for the excitation cross sections. In e-N_2, vibrational effects are important in the Σ_g symmetry and so affect the elastic cross section as well. This system also provides a laboratory to demonstrate the practical advantages of using vibrational averaging to reduce the number of partial waves required for convergence.

ACKNOWLEDGMENTS

The authors would like to thank Dr. Barry Schneider who, during a vigorous discussion following a colloquium one of us (M.A.M.) gave at Los Alamos, encouraged us to pursue quantitatively the ideas of this paper. We are also grateful to Dr. Greg Snitchler, who calculated many of the separable-exchange BFVCC numbers used as benchmarks, and to Dr. Grahame Danby for a careful reading of a preliminary version of this manuscript. This research was supported by a grant from the National Science Foundation, Grant No. PHY-8505438, and utilized the CRAY 2 and XMP system at the National Center for Supercomputing Applications at the University of Illinois at Urbana-Champaign.

[1]M. A. Morrison, Adv. At. Mol. Phys. **24**, 51 (1988).

[2]For a tutorial-style introduction to electron-molecule collision theory see M. A. Morrison, Aust. J. Phys. **36**, 239 (1983).

[3]For a technical overview of these approximations see B. D. Buckley, P. G. Burke, and C. J. Noble, in *Electron-Molecule Collisions,* edited by I. Shimamura and K. Takayanagi (Plenum, New York, 1984), p. 495.

[4]A particularly useful overview of R-matrix theory appears in P. G. Burke, in *Quantum Dynamics of Molecules,* edited by R. G. Wooley (Plenum, New York, 1980), p. 483.

[5]For a survey of applications of these methods through 1979 see N. F. Lane, Rev. Mod. Phys. **52**, 29 (1980).

[6]M. A. Morrison and B. C. Saha, Phys. Rev. A **34**, 2786 (1986).

[7]R. J. W. Henry, Phys. Rev. A **2**, 1349 (1970).

[8]N. Chandra and A. Temkin, Phys. Rev. A **13**, 188 (1976).
[9]M. A. Morrison, A. N. Feldt, and B. C. Saha, Phys. Rev. A **30**, 2811 (1984).
[10]F. H. M. Faisal and A. Temkin, Phys. Rev. Lett. **28**, 203 (1972); A. Temkin and E. C. Sullivan, *ibid.* **33**, 1057 (1974).
[11]A. Klonover and U. Kaldor, J. Phys. B **12**, L61 (1979).
[12]See, for example, M. A. Morrison, N. F. Lane, and L. A. Collins, Phys. Rev. A **15**, 2186 (1977).
[13]For an illustration of this point in the context of converging RR e-N_2 scattering calculations see M. A. Morrison, in *Electron Molecule and Photon-Molecule Collisions,* edited by T. N. Rescigno, V. McKoy, and B. I. Schneider (Plenum, New York, 1979), p. 15.
[14]W. H. Press, B. P. Flannery, S. A. Teukolsky, and W. T. Vetterling, *Numerical Recipes: The Art of Scientific Computing* (Cambridge University Press, New York, 1986), p. 629.
[15]A number of programs for easy, accurate calculation of these potentials are available through the Computer Physics Communications Program Library; for diatomic targets see M. A. Morrison, Comput. Phys. Commun. **21**, 63 (1980); L. A. Collins, D. W. Norcross, and G. B. Schmid, *ibid.* **21**, 79 (1980).
[16]A. Temkin and K. V. Vasavada, Phys. Rev. **160**, 190 (1967); S. Hara, J. Phys. Soc. Jpn. **27**, 1592 (1969).
[17]D. M. Chase, Phys. Rev. A **104**, 838 (1956); E. S. Chang and U. Fano, *ibid.* **6**, 173 (1972); M. Shugard and A. U. Hazi, *ibid.* **12**, 1975 (1975).
[18]M. A. Morrison, A. N. Feldt, and D. A. Austin, Phys. Rev. A **29**, 2518 (1984).
[19]A. M. Arthurs and A. Dalgarno, Proc. R. Soc. London Ser. A **256**, 540 (1960).
[20]For application of the LFCC method in the RR approximation to e-H_2 collisions see N. F. Lane and S. Geltman, Phys. Rev. **160**, 53 (1967); R. J. W. Henry and N. F. Lane, *ibid.* **183**, 221 (1969).
[21]Note that the tilde atop the radial wave function $\tilde{u}^{\Lambda}_{l,l_0}(r)$ implies that it is the solution of the VIBAV equations; i.e., this function is *not* $\langle\phi_0|u^{\Lambda}_{l,l_0}(r;R)|\phi_0\rangle$.
[22]G. Raseev, Comput. Phys. Commun. **20**, 275 (1980); A. L. Sinfailam, *ibid.* **1**, 445 (1970).
[23]Programs to evaluate differential and integrated cross sections from BFFN scattering matrices include M. A. Brandt, D. G. Truhlar, and R. L. Smith, Comput. Phys. Commun. **5**, 456 (1973); K. Onda, D. G. Truhlar, and M. A. Brandt, *ibid.* **21**, 97 (1980); S. A. Salvini, *ibid.* **27**, 25 (1982); S. A. Salvini and D. G. Thompson, *ibid.* **22**, 49 (1981); R. J. W. Henry, *ibid.* **10**, 375 (1975).
[24]See Eq. (37) of Ref. 1.
[25]The most widely used model exchange potential in electron-molecule scattering is based on a free-electron-gas approximation. See M. A. Morrison and L. A. Collins, Phys. Rev. A **23**, 127 (1981).
[26]A related model potential for correlation effects is explored in J. K. O'Connell and N. F. Lane, Phys. Rev. A **27**, 1893 (1983). For applications of this potential see N. T. Padial and D. W. Norcross, *ibid.* **29**, 1742 (1984); **29**, 1590 (1984); N. T. Padial, *ibid.* **32**, 1379 (1985); A. Jain and D. W. Norcross, *ibid.* **32**, 134 (1985); J. Chem. Phys. **84**, 739 (1986); P. K. Bhattacharyya, D. L. Syamal, and B. C. Saha, Phys. Rev. A **32**, 854 (1985).
[27]See, for example, Sec. II.4 and Fig. 14 of Ref. 2.
[28]J. W. Moskowitz and L. C. Snyder, in *Methods of Electronic Structure Theory,* edited by H. F. Schaeffer, III (Plenum, New York, 1977), p. 387.
[29]T. Dunning, J. Chem. Phys. **55**, 3958 (1971).
[30]T. L. Gibson and M. A. Morrison, Phys. Rev. A **29**, 2497 (1984).
[31]M. A. Morrison and P. J. Hay, Phys. Rev. A **20**, 740 (1979).
[32]M. A. Morrison, B. C. Saha, and T. L. Gibson, Phys. Rev. A **36**, 3682 (1987).
[33]Bidhan C. Saha, in *Electron-Molecule Scattering and Photoionization,* edited by P. G. Burke and J. B. West (Plenum, New York, 1988), p. 221.
[34]W. Kolos and C. C. Roothaan, Rev. Mod. Phys. **32**, 205 (1960); L. Laaksonen, P. Pyykko, and D. Sundholm, Int. J. Quant. Chem. **23**, 319 (1983).
[35]P. A. Christiansen and E. A. McCullough, Jr., J. Chem. Phys. **55**, 439 (1978).
[36]Actually, the minimum of our near-HF ground state curve for N_2 occurs at $R=2.02a_0$; the HF electronic energy at this R is $-108.9766E_h$.
[37]K. B. MacAdam and N. F. Ramsey, Phys. Rev. A **6**, 898 (1972).
[38]W. Kolos and L. Wolniewicz, J. Chem. Phys. **46**, 1426 (1967).
[39]A. C. Newell and R. C. Baird, J. Appl. Phys. **36**, 3751 (1965).
[40]N. J. Bridge and A. D. Buckingham, Proc. R. Soc. London Ser. A **295**, 334 (1966).
[41]R. H. Orcutt and R. H. Cole, J. Chem. Phys. **46**, 697 (1967); T. M. Miller and B. Bederson, Adv. At. Mol. Phys. **13**, 1 (1978).
[42]See Eq. (16) of Ref. 32 for the form of this kernel and Table II of this paper for details on the convergence of its calculation for e-N_2.
[43]T. N. Rescigno and A. E. Orel, Phys. Rev. A **24**, 1267 (1981); L. A. Collins and B. I. Schneider, *ibid.* **34**, 1564 (1986).
[44]G. Snitchler, D. Norcross, S. Alston, B. Saha, and M. Morrison, in *Abstracts of the XVI International Conference on the Physics of Electronic and Atomic Collisions, New York, 1989,* edited by P. G. Burke and J. B. West (Plenum, New York, 1989), p. 304.
[45]A. Temkin, Phys. Rev. **107**, 1004 (1957).
[46]T. L. Gibson, Ph.D thesis, University of Oklahoma, 1982.
[47]T. L. Gibson and M. A. Morrison, J. Phys. B **14**, 727 (1981).
[48]B. I. Schneider and L. A. Collins, Phys. Rev. A **27**, 2847 (1983).
[49]A. A. Radzig and B. Smirnov, *Reference Data on Atoms, Molecules, and Ions* (Springer-Verlag, New York, 1986).
[50]G. Simons, R. G. Parr, and J. M. Finlan, J. Chem. Phys. **59**, 3229 (1973); J. M. Finlan and G. Simons, J. Mol. Spectrosc. **57**, 1 (1975).
[51]G. A. Parker, Ph.D thesis, Brigham Young University, 1976.
[52]E. S. Chang and A. Temkin, Phys. Rev. A **23**, 399 (1969).
[53]A. N. Feldt and M. A. Morrison, Phys. Rev. A **29**, 401 (1984).
[54]The error introduced by these approximate treatments of vibrational effects depends to some extent on how one treats exchange. We carried out a comparison similar to the one reported in this section in which we approximated exchange effects via a "tuned" free-electron-gas model potential. At 5.0 eV, for example, the RR approximation introduces errors of 7% in the exact-exchange $\sigma_{0\to2}$ and 10% in the approximate-exchange cross section. The VIBAV approximation reduces these errors to 1% and 2%, respectively.
[55]J. P. England, M. T. Elford, and R. W. Crompton, Aust. J. Phys. **41**, 573 (1988).
[56]J. Ferch, W. Raith, and J. Schroder, J. Phys. B **13**, 1481 (1980).
[57]G. Dalba, P. Fornasini, I. Lazzizzera, G. Ranieri, and A. Zecca, J. Phys. B **13**, 2839 (1980).
[58]R. K. Jones, J. Chem. Phys. **82**, 5424 (1985).